OXFORD

International Journal of Neuropsychopharmacology (2018) 21(6): 603–615

doi:10.1093/ijnp/pyy022
Advance Access Publication: March 5, 2018
Regular Research Article

REGULAR RESEARCH ARTICLE

A Critical Role of Mitochondria in BDNF-Associated Synaptic Plasticity After One-Week Vortioxetine Treatment

Fenghua Chen, Jibrin Danladi, Maryam Ardalan, Betina Elfving, Heidi K. Müller, Gregers Wegener, Connie Sanchez, Jens R. Nyengaard

Translational Neuropsychiatry Unit, Department of Clinical Medicine, Aarhus University, Risskov, Denmark (Drs Chen, Danladi, Ardalan, Elfving, Müller, Wegener, and Sanchez); Core Center for Molecular Morphology, Section for Stereology and Microscopy, Department of Clinical Medicine, Aarhus University, Aarhus, Denmark (Drs Chen and Nyengaard); Centre for Stochastic Geometry and Advanced Bioimaging, Aarhus University, Aarhus, Denmark (Dr Nyengaard); Alkermes, Biotechnology, Waltham, MA (Dr Sanchez); Center of Excellence for Pharmaceutical Sciences, North-West University, Potchefstroom, South Africa (Dr Wegener); Department of Clinical Medicine - Center of Functionally Integrative Neuroscience, Aarhus University, Aarhus, Denmark (Dr Ardalan); AUGUST Centre, Department of Clinical Medicine, Aarhus University, Risskov, Denmark (Dr Wegener)

Shared authorship (Drs Sanchez and Nyengaard).

Correspondence: Fenghua Chen, Department of Clinical Medicine - Translational Neuropsychiatry Unit, Skovagervej 2, 8240 Risskov, Denmark (fenghua.chen@clin.au.dk).

Abstract

Background: Preclinical studies have indicated that antidepressant effect of vortioxetine involves increased synaptic plasticity and promotion of spine maturation. Mitochondria dysfunction may contribute to the pathophysiological basis of major depressive disorder. Taking into consideration that vortioxetine increases spine number and dendritic branching in hippocampus CA1 faster than fluoxetine, we hypothesize that new spines induced by vortioxetine can rapidly form functional synapses by mitochondrial support, accompanied by increased brain-derived neurotrophic factor signaling.
Methods: Rats were treated for 1 week with vortioxetine or fluoxetine at pharmacologically relevant doses. Number of synapses and mitochondria in hippocampus CA1 were quantified by electron microscopy. Brain-derived neurotrophic factor protein levels were visualized with immunohistochemistry. Gene and protein expression of synapse and mitochondria-related markers were investigated with real-time quantitative polymerase chain reaction and immunoblotting.
Results: Vortioxetine increased number of synapses and mitochondria significantly, whereas fluoxetine had no effect after 1-week dosing. BDNF levels in hippocampus DG and CA1 were significantly higher after vortioxetine treatment. Gene expression levels of *Rac1* after vortioxetine treatment were significantly increased. There was a tendency towards increased gene expression levels of *Drp1* and protein levels of Rac1. However, both gene and protein levels of c-Fos were significantly decreased. Furthermore, there was a significant positive correlation between BDNF levels and mitochondria and synapse numbers.
Conclusion: Our results imply that mitochondria play a critical role in synaptic plasticity accompanied by increased BDNF levels. Rapid changes in BDNF levels and synaptic/mitochondria plasticity of hippocampus following vortioxetine compared with fluoxetine may be ascribed to vortioxetine's modulation of serotonin receptors.

Keywords: synapse, mitochondria, BDNF, depression, vortioxetine

Received: January 30, 2018; **Revised:** February 26, 2018; **Accepted:** March 2, 2018

Significance Statement

Preclinical studies have indicated that the antidepressant effect of vortioxetine involves increased synaptic plasticity and promotion of spine maturation. Mitochondria dysfunction may contribute to the pathophysiological basis of major depressive disorder. The interplay between mitochondria and synapses has been less well studied. In the present study, our results indicate that mitochondria play a critical role in synaptic plasticity accompanied by increasing BDNF levels. In particular, the coincidence of rapid changes in the BDNF levels and synaptic/mitochondria plasticity of hippocampus following vortioxetine compared with fluoxetine may be ascribed to vortioxetine's modulation of one or more serotonin receptors. Moreover, gene and protein expression related to the link between the mitochondria and synapses may possibly offer a molecular mechanism explanation in response to vortioxetine treatment.

Introduction

The multimodal antidepressant vortioxetine is an antagonist at 5-HT_3, 5-HT_7, and 5-HT_{1D} receptors, a partial agonist at 5-HT_{1B} receptors, an agonist at 5-HT_{1A} receptors, and a serotonin transporter (SERT) inhibitor (Sanchez et al., 2015). The procognitive effects of vortioxetine in preclinical rodent models and also improvement of certain aspects of cognitive function in major depressive disorder (MDD) patients have been documented (Frampton, 2016; Li et al., 2017). Preclinical studies in rodents indicate that vortioxetine's effects on synaptic transmission, neurogenesis, dendritic branching, and dendritic spine maturation differ significantly from a selective serotonin reuptake inhibitor (SSRI) (Dale et al., 2014; Waller et al., 2016). Furthermore, several lines of evidence reveal that vortioxetine can promote expression of various genes that play a role in synaptic plasticity (du Jardin et al., 2016; Waller et al., 2016). We have previously reported that 1-week vortioxetine treatment induced changes in spine number and dendritic morphology, whereas an equivalent dose of fluoxetine had no effects (Chen et al., 2016). In the central nervous system, most excitatory postsynaptic terminals reside in dendritic spines. Spine remodeling is usually associated with changes in synaptic connectivity. However, we do not know whether the rapid induction of new spines by vortioxetine form functional synapses and react to presynaptic stimulation. Therefore, we conducted further studies to demonstrate changes of excitatory synapses located on dendritic spines after vortioxetine treatment using electron microscopy.

Moreover, several lines of preclinical and clinical evidence indicate that vortioxetine can enhance cognitive function via modulation of a wide range of neurotransmitters (Sanchez et al., 2015; Pehrson et al., 2016; Li et al., 2017; Pan et al., 2017; Smith et al., 2017). Pathophysiological processes in MDD are intimately linked to the biological underpinnings of cognitive loss (Anderson, 2018). The various pathophysiological changes, such as increased oxidative stress, occurring over the course of neuroprogression in MDD may lead to suboptimal mitochondrial functioning (Anderson, 2018; Czarny et al., 2018). Suboptimal mitochondrial functioning may be the primary driver of the pathophysiological changes and emerging cognitive deficits in MDD (Anderson, 2018). Substantial data support that MDD was accompanied by oxidative stress dysregulation, which could indicate a dysfunction of mitochondria, and that antidepressant treatment may reduce oxidative stress (Alcocer-Gomez et al., 2014; Klinedinst and Regenold, 2015). Increased production of reactive oxygen species (ROS) associated with age- and disease-dependent loss of mitochondrial function, altered metal homeostasis, and reduced antioxidant defense directly affect synaptic activity and neurotransmission in neurons leading to cognitive dysfunction (Vavakova et al., 2015; Czarny et al., 2018). Synapses are dynamic, and mitochondria constantly move along axons and dendrites by dividing and fusing in response to synaptic changes to regulate synaptic activity. Importantly, the activity of synapses differentially influences the mitochondrial morphology and distribution between axons and dendrites (Chang et al., 2006). Therefore, mitochondria not only provide dynamic energy support for normal synaptic functioning but also directly modulate synaptic structural and functional plasticity.

The interplay between mitochondria and synapses has been less well studied. Based on our previous observation that vortioxetine increased spine number and dendritic branching in the hippocampus CA1 faster than the SSRI fluoxetine, we hypothesize that the concomitant function of mitochondria and brain-derived neurotrophic factor (BDNF)-signaling is necessary for rapid adaptive synaptic plasticity by vortioxetine. Identification of molecular mechanisms related to the link between the mitochondria and synapses in response to vortioxetine treatment may aid in a better understanding of their therapeutic capacity.

Materials and Methods

Animals

Adult male Sprague-Dawley rats (180–200 g) (n = 42) were kept on a normal light:dark cycle with free access to food and water. There were 6/8 rats (6 for morphological and 8 for molecular studies) in each group (vortioxetine, fluoxetine, and vehicle). All rats were handled for 7 d before any treatment was initiated.

Antidepressant Treatment

Vortioxetine was given in chow (1.6 g/kg food, provided by H. Lundbeck A/S) for 7 d. This dosage has previously been shown to produce >80% SERT occupancy (Chen et al., 2016). Fluoxetine, also provided by H. Lundbeck A/S, was delivered in the drinking water (160 mg/L) for 7 d. This dose was chosen to achieve >80% SERT occupancy with fluoxetine (Chen et al., 2016). Regular food pellets with the same composition were given to vehicle rats for the same period. Drug delivery via the chow ensures a stable target engagement and removed any stressors associated with dosing. Body weight, food intake, and fluid intake were measured regularly. All procedures are approved by the Danish animal ethics committee (2012-15-2934-00254; C –sheet 1).

Tissue Preparation and Sampling

Rats were perfused transcardially 24 h after treatment with fixatives (4% paraformaldehyde and 2% glutaraldehyde in 0.1 M PBS). Brains were removed and postfixed in the same fixative, and kept at 4°C until further processing. Hippocampi were isolated, and left or right hippocampus was selected randomly, manually straightened along the septotemporal axis to diminish its natural curvature, embedded in 5% agar, and cut into 65-µm-thick sections perpendicularly to its longest axis on a Vibratome 3000.

Three sets of sections were chosen based on a systematic random sampling principle and a section sampling fraction of 1/15. One set was stained with thionin for estimating the volume of hippocampus with light microscopy and immunohistochemically staining for BDNF was performed on a second set. The last set of tissue sections for electron microscopy was embedded in TAAB 812 Epon (TAAB) for cutting 20 consecutive serial ultrathin sections. The actual mean ultrathin section thickness (around 67–72 nm) was determined according to Small's method of minimal folds (Small JV, 1968).

Ultrastructural Study of Synapses and Mitochondria

The ultrathin sections were observed in a FEI Morgagni transmission electron microscope. Electron micrographs were taken with a digital camera at an initial magnification of 10 500×, and digitally enlarged to a final magnification of 23 850×. The synapses and mitochondria were sampled by the physical disector and analyzed using the digitized electron micrographs via iTEM software (Olympus Soft Imaging Solutions GmbH) (Chen et al., 2010).

The synapses were identified primarily on the basis of the presence of a postsynaptic density (PSD) with vesicles in close proximity to the presynaptic zone. Only spine and shaft synapses of asymmetric synapses were analyzed in this study. In the spine synapses, PSD located on the spines that were small spherical postsynaptic protrusions of the dendrite filled with a clear cytoplasmic matrix and a distinct spine apparatus but without mitochondria and microtubules. The shaft synapses terminated directly on the dendritic shaft. The dendrites were differentiated from spines by a less densely stained cytoplas containing microtubules and mitochondria. The spine synapses may be subdivided into perforated and nonperforated synapses. Perforated synapses displayed discontinuous or perforated PSD profiles, whereas nonperforated synapses exhibited continuous PSD files in all consecutive sections (Figure 1) (Geinisman et al., 2001).

The synapse number density was estimated using the PSD as a counting unit. At least 2 neuropil fields were randomly photographed on each ultrathin section. From each section series (16–20 sections), 10 consecutive sections were selected from section 2 (section 1 was look-up section) and used as the reference section of the disectors. The last 5 sections of each series were used as look-up sections to ensure that all counted PSDs were included in their entirety in the section series. Axo-spinous perforated synapses and shaft synapses were counted with ~120 disectors and axo-spinous nonperforated synapses with ~48 disectors in each animal. The total synapse number was estimated as the product of the synapse number density and volume of the CA1 stratum radiatum. Detailed information can be found in our previous paper (Chen et al., 2010).

Mitochondria were counted throughout the neuropil and specifically in the axon terminals and dendrites. The criteria for identifying mitochondria were the presence of distinctive cristae and a double membrane (Figure 1). Neuropil structures were identified as axon terminals (presence of 3 or more synaptic vesicles), dendrites (postsynaptic to a synapse or having an attached spine), or astroglial processes (presence of fibrils and watery cytoplasm). The total number of mitochondria in neuropil and the number of mitochondria in axon terminals and dendrites were determined.

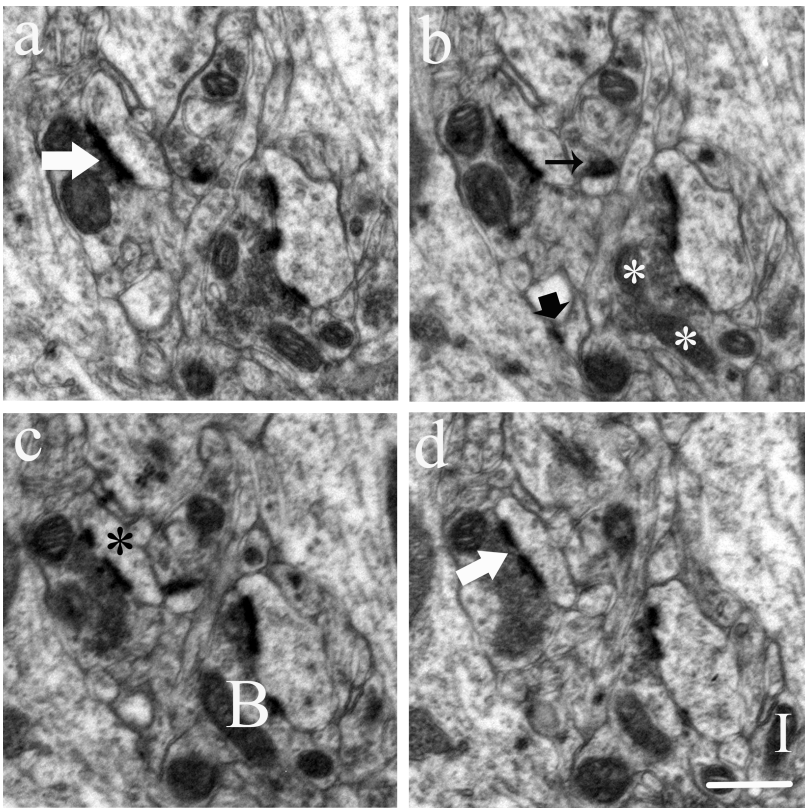

Figure 1. Count of synapses and mitochondria in serial sections. Electron micrographs of consecutive ultrathin sections (a–d) showed nonperforated synapses (black arrow), a perforated synapse (large white arrow), and shaft synapse (large black arrow). The postsynaptic spine exhibited PSD discontinuities (black stars). Mitochondria: Isolated particle (I), A branch dividing (white stars), or branches connection (B). Scale bar, 0.5 μm.

Combining the disector principle with the object's 3D Euler number estimates the number of mitochondria (Kroustrup and Gundersen, 2001). In terms of disector section pairs, mitochondria profiles in one section plane are compared with mitochondria profiles on the next section plane. Mitochondria are identified in each section plane, and a change between planes is deduced as being 1 of 2 significant possibilities: a new isolated part, a so-called "Island," *I*, or a new connection between isolated mitochondria, a "Bridge," *B*, in an existing mitochondrion. The total Euler number, Σx, contribution from all disectors is obtained as the signed sum of Islands, and Bridges (Figure 1). The total mitochondria number was estimated as the product of the mitochondria number density and volume of CA1 stratum radiatum. Detailed information can be found in our previous paper (Chen et al., 2013).

Immunohistochemistry

Free-floating 8–9 vibratome sections from each animal were washed 3 times for 10 min in Tris-buffered saline (TBS) (pH 7.4), immersed in endogenous peroxidase blocking solution for 30 min, and were incubated in preheated Target Retrieval solution at 85°C for 40 min (Dako, EnVision System HRP). Tissue sections were then incubated at 4°C overnight in a solution containing the rabbit anti-BDNF polyclonal antibody (diluted 1: 500) (AB1779, Merck Millipore). The next day, sections were washed 3 times for 10 min with buffer (1% BSA and 0.3% Triton-X in TBS) and incubated in buffer (1% BSA in TBS) added goat anti-rabbit IgG (1:200) for 2 h at room temperature. Sections were washed 3 times for 10 min in TBS and then visualized with 0.1% 3, 3'-diaminobenzidine containing 0.3% H_2O_2 in TBS for 7 min and washed by TBS 3 times for 10 min. Sections were then mounted on the gelatin-coated slides and dehydrated with alcohol gradient and cleared with xylene.

Images of whole immunostained sections were taken by the Virtual Slides System VS120 (Olympus) including the software VS ASW OIL 2.7 (Olympus Soft Imaging Solutions GmbH). ImageJ software was used to analyze the images of immunostained sections and calculated the mean optical density of BDNF-positive areas in subregions of hippocampus (Figure 2).

Measurement of mRNA Levels with Real-time Quantitative Polymerase Chain Reaction (Real-Time qPCR)

The rats were decapitated and the brain collected. Briefly, coronal brain sections (200 µm) were cut using a cryostat at -20°C. Using a scalpel, the CA1 area was dissected and stored at -80°C until extraction of RNA with the Qiagen Rneasy Mini kit (Qiagen) as previously described (Silva Pereira et al., 2017). The dissected CA1 tissues were homogenized in Lysis buffer (Qiagen) with a mixer-mill (Retsch; twice for 40 s at 30 Hz/s). Total RNA was isolated following the manufacturer's instructions (Qiagen). The RNA concentration, A260/280, and A260/230 ratios were determined with a NanoDrop spectrometer (Thermo Fisher Scientific). Afterwards, RNA was reversely transcribed using random primers and Superscript IV Reverse Transcriptase (Invitrogen) following the manufacturer's instructions. The input RNA concentration was adjusted to 29 ng/µL in the individual samples. The cDNA samples were stored undiluted at -80°C until real-time qPCR analysis.

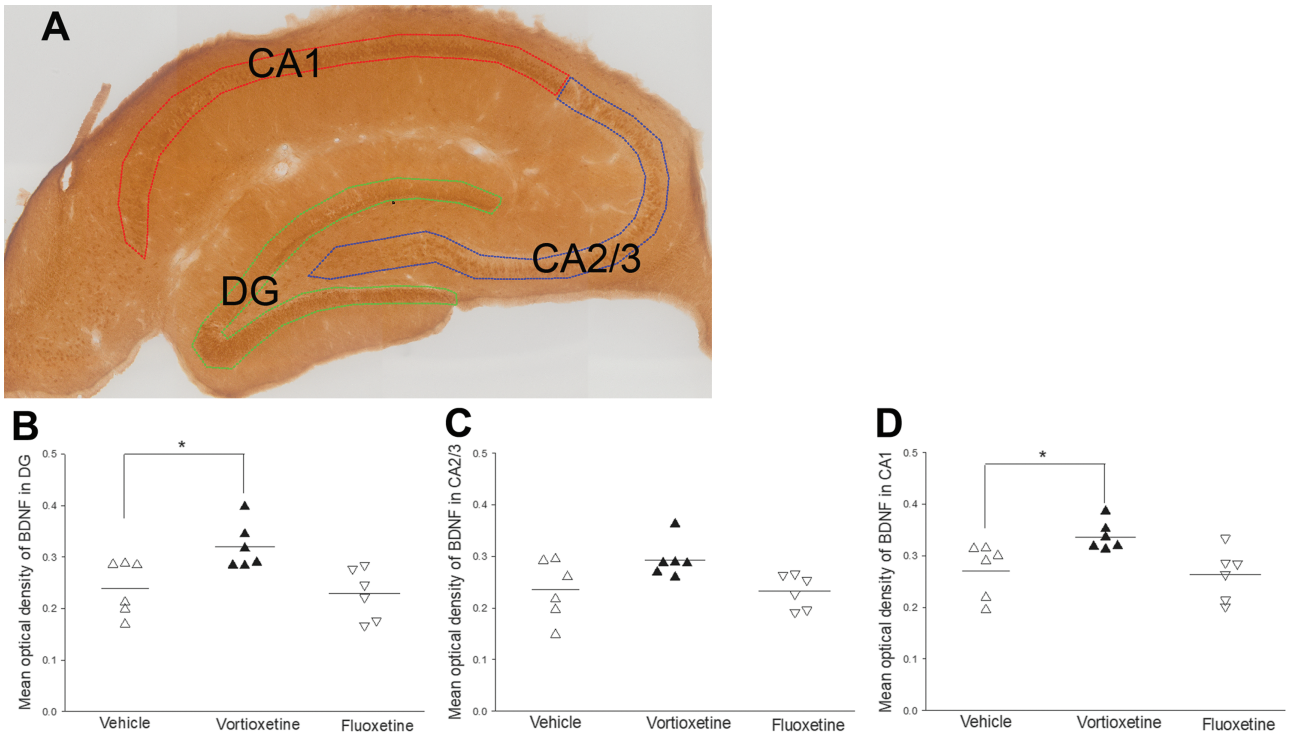

Figure 2. (A) BDNF expression levels were examined by immunohistochemistry in the subregions of hippocampus. (B–D) Immunohistochemistry-examined BDNF expression levels in each group. Mean optical density (MOD) was calculated with the following formula: OD = log10(max pixel intensity/mean pixel intensity), where max pixel intensity = 255. MOD in the vortioxetine-treated group significantly increased compared with the vehicle and fluoxetine groups in DG (A) and CA1 (C) subregions of hippocampus.

Real-Time qPCR

The samples were diluted 1:10 with DEPC water before being used as a qPCR template. The real-time qPCR reactions were carried out in 96-well PCR-plates using an Mx3005P (Stratagene) and SYBR Green. The gene expression of synapse-related genes (*Arc*, *Cdc42*, *c-fos*, *Cofilin1*, *Homer1*, *Psd95*, *Rac1*, *RhoA*, *Spinophilin*, *Synapsin1*), mitochondria-related genes (*Drp1*, *Fis1*, *Mfn1*, *Mfn2*, *Opa1*), as well as 8 different reference genes (*18s rRNA*, *ActB*, *CycA*, *Gapdh*, *Hmbs*, *Hprt1*, *Rpl13A*, *Ywhaz*) was investigated. The reference genes were selected as previously described (Bonefeld et al., 2008). The primers were designed and tested as in our previous work (Elfving et al., 2008). Essential gene-specific data about primer sequence and amplicon sizes is given in Supplement Table 1. The primers were obtained from Sigma-Aldrich. Each SYBR Green reaction (10 µL total volume) contained 1x SYBR Green master mix (Sigma-Aldrich), 0.5 µM primer pairs, and 3 µL of diluted cDNA and were carried out as described previously (Elfving et al., 2008, 2010). The mixture was heated initially to 95°C for 3 min to activate hot-start iTaq DNA polymerase and then 40 cycles with denaturation at 95°C for 10 s, annealing at 60°C for 30 s, and extension at 72°C for 60 s were applied. To verify that only one PCR product was detected, the samples were subjected to a heat dissociation protocol; after the final cycle of the PCR, the reactions were heat-denatured by increasing the temperature from 60°C to 95°C. All samples and the standard curve were run in duplicates. A standard curve was generated on each plate.

Initially, the mRNA levels were determined for the 8 reference genes. Stability comparison of the expression of the reference genes was then conducted with the Normfinder software. Values of the target genes were subsequently normalized with the geometric mean of the 2 optimal reference genes (*Ywhaz* and *Hmbs*), based on the NormFinder mathematical algorithm (Andersen et al., 2004).

Immunoblotting

Aliquots (20 µg total protein) of hippocampal CA1 tissue homogenized in Cell Lysis Buffer (Bio-Rad) containing 1x protease inhibitor cocktail (Roche) were separated on 10% criterion TGX gels (Bio-Rad), transferred to nitrocellulose membranes, blocked in odyssey blocking buffer (Licor), and probed with the primary antibodies: mouse anti-Rac1 (Abcam ab33186; 1:500), mouse anti-Drp1 (Cell Signaling #14647; 1:1000), rabbit anti-c-Fos (Cell Signaling #2250; 1:500), and rabbit anti-β-actin (Licor 926–42212; 1:3000) overnight at 4°C followed by incubation with the appropriate IRDye conjugated secondary antibody for 1 h at RT: IRDye 800CW goat anti-mouse IgG, IRDye 680RD goat anti-rabbit, or IRDye 800CW goat-anti rabbit IgG, at 1:15 000 dilution (Licor). Infrared signals were detected using the Odyssey CLx infrared imaging system, and bands were quantified using Image Studio software (LI-COR Biosciences). Band intensities were normalized to β-actin levels within the same lane.

Statistical Procedures

All data were subjected to 1-way ANOVA to compare treatment responses followed by posthoc tests (Tukey and least significant difference) and Dunnett's test for multiple comparisons (Immunoblotting). $P < .05$ was considered statistically significant. Statistical analyses and graphical representations of the findings were carried out using SPSS11 (SPSS Corp) and Sigmaplot 10 (SYSTAT Inc.) software.

Results

BDNF Expression Levels by Immunohistochemistry

BDNF immunoreactivity was mainly localized in the intra-cytoplasm of neurons. Mean optical density of BDNF in DG and CA1 ($P < .05$) of hippocampus was significantly higher in rats treated with vortioxetine compared with vehicle rats (Figure 2). There was no difference between the fluoxetine-treated rats and vehicle rats.

The Volume of Hippocampus and Hippocampal CA1 Stratum Radiatum

The volume of whole hippocampus and hippocampal CA1-SR in the vortioxetine group was significantly increased compared with the vehicle group ($P < .05$) (Figure 3; Table 1). There was no difference in fluoxetine-treated rats compared with vehicle rats.

The Number of Synapses in Serial Sections

The total number of synapses ($P < .001$), nonperforated spine synapses ($P < .01$), and perforated spine synapses ($P < .01$) was significantly increased in the vortioxetine group compared with the fluoxetine and vehicle groups. No changes in the number of shaft synapses were observed (Figure 4; Table 1).

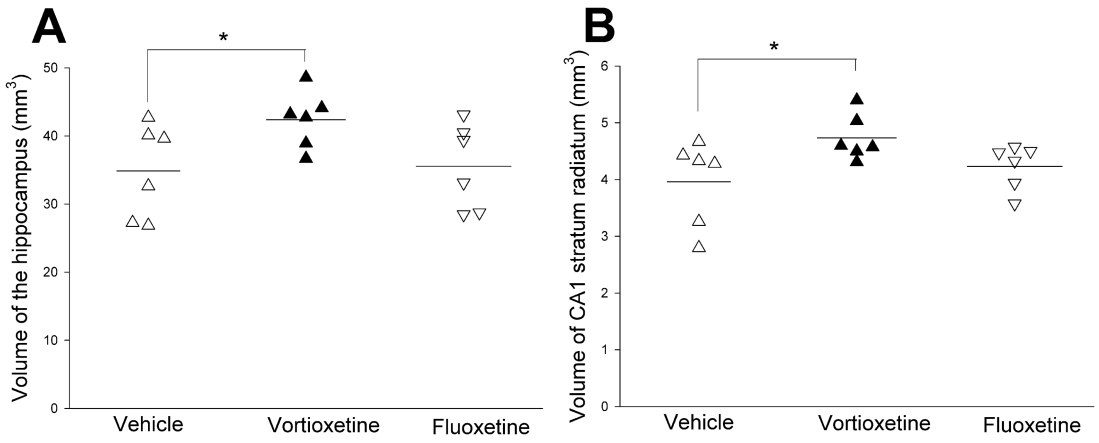

Figure 3. The volume of hippocampus and CA1 stratum radium. The volume of hippocampus and CA1-SR in vortioxetine group is significantly increased compared with the vehicle and fluoxetine groups (*$P < .05$).

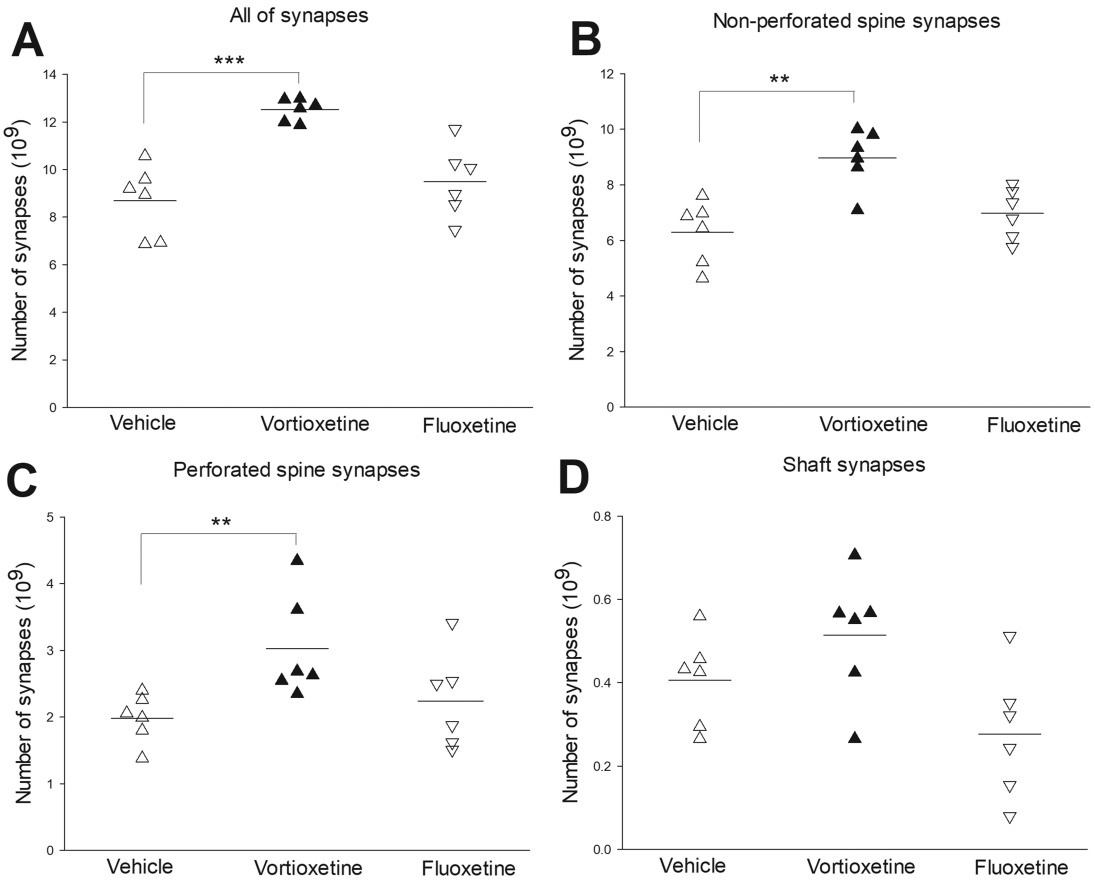

Figure 4. The number of synapses including subtypes of synapse in CA1 (*P < .05; **P < .01; ***P < .001) (Δ: vehicle group; ▲: vortioxetine; ▽: fluoxetine). (A) The total number of synapses was significantly higher in the vortioxetine group compared with the vehicle and fluoxetine groups. (B) The number of nonperforated spine synapses was significantly higher in vortioxetine group compared with the vehicle and fluoxetine groups. (C) The number of perforated spine synapses was significantly higher in the vortioxetine group compared with the vehicle and fluoxetine groups. (D) The number of shaft synapses was not any different in the vortioxetine group compared with the vehicle and fluoxetine groups.

The Number of Mitochondria in Serial Sections and Mitochondria Volume

The mitochondria number in total neuropil ($P < .05$) and axon terminal ($P < .05$) was significantly increased in the vortioxetine group compared with fluoxetine and vehicle groups. There were no significant differences in mitochondria volume and the dendrites' mitochondria number (Figure 5; Table 1).

Synapse- and Mitochondria-Related Gene Expression and Protein Levels

Real-time qPCR analysis revealed that *Rac1* in the vortioxetine treatment group was significantly increased compared with the vehicle group ($P < .05$) (Figure 6). There was no significant difference in mRNA levels of *Rac1* in the fluoxetine treatment group compared with the vehicle group. There was a tendency towards increased mRNA levels of *Drp1* in the vortioxetine treatment group compared with vehicle group. The mRNA expression levels of the immediate early gene (IEG), *c-fos*, were significantly reduced following vortioxetine ($P < .01$) and fluoxetine ($P < .05$) treatment relative to vehicle; however, neither vortioxetine nor fluoxetine had any effect on *Arc* mRNA expression. The other selected synapse-related and mitochondria-related genes given in Supplement Table 1 were not regulated.

The protein expression levels of c-Fos were significantly reduced following vortioxetine ($P < .05$) and fluoxetine ($P < .01$) treatment relative to vehicle. There was a tendency towards increase of protein expression levels of Rac1 in the vortioxetine treatment group compared with vehicle group. No changes of the protein levels of Rac1 in the fluoxetine treatment group were observed. There were no significant differences in protein expression levels of Drp1 in the vortioxetine and fluoxetine treatment groups compared with vehicle group (Figure 7).

Correlations between Synapses, Mitochondria, Volume, and BDNF Level in the Hippocampus following Antidepressant Treatment

Correlations of morphological data and BDNF values are shown in Figure 8. BDNF levels were positively correlated with the volume of hippocampal CA1-SR ($r = 0.80$; $P < .001$), synapse number ($r = 0.78$; $P < .001$), and mitochondrial number ($r = 0.76$; $P < .001$). Moreover, the volume of hippocampal CA1-SR was positively correlated with synapse number ($r = 0.78$; $P < .001$) and mitochondrial number ($r = 0.61$; $P < .001$). Furthermore, there was a positive correlation between total mitochondria number and total number of synapses ($r = 0.81$; $P < .001$).

Discussion

Here, we have shown that vortioxetine significantly increased the number of synapses and mitochondria accompanied by BDNF level elevation, whereas fluoxetine had no effect after 7

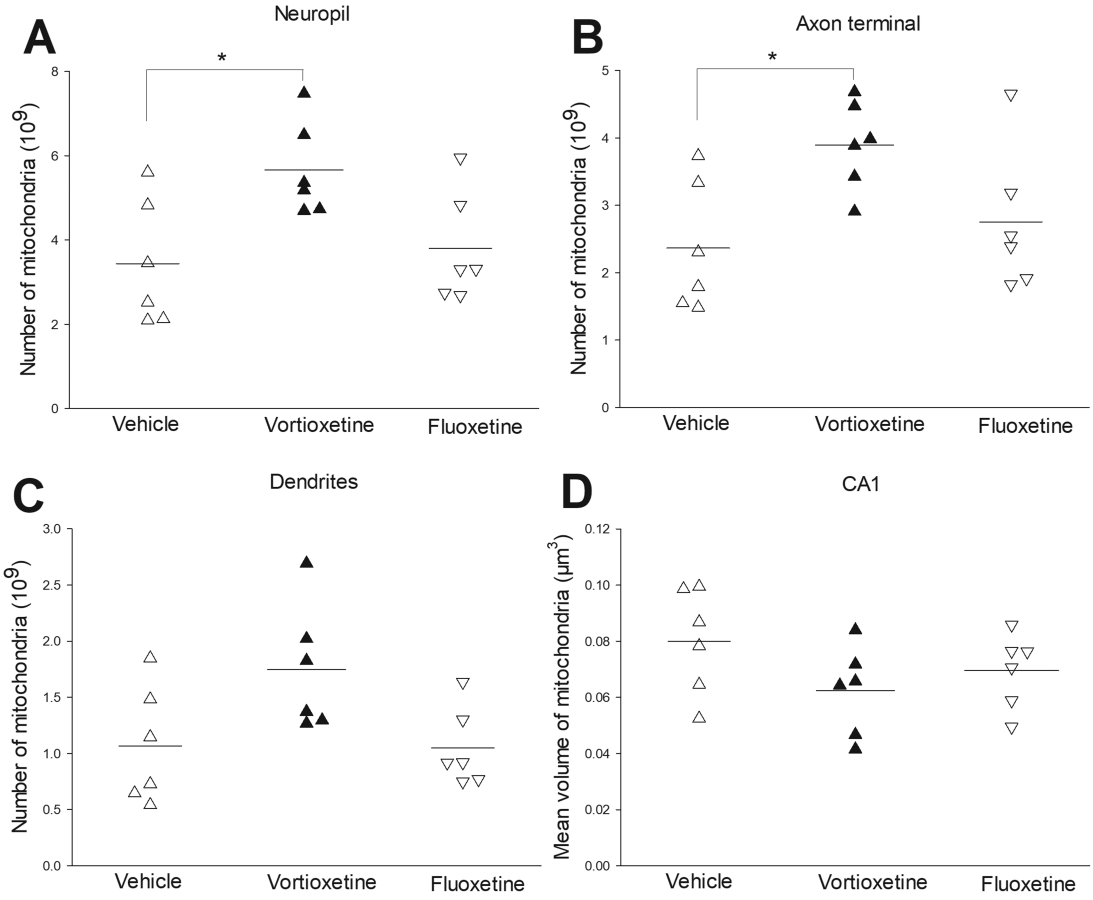

Figure 5. The number of mitochondria in the various structures (neuropil, axons, and dendrites) and the mean volume of mitochondria in CA1 (*, $P < .05$) (Δ: vehicle group; ▲: vortioxetine; ▽: fluoxetine). (A) The total number of mitochondria in neuropil displayed a significant increase in the vortioxetine group compared with the vehicle and fluoxetine groups. (B) The number of mitochondria in the axon terminal also showed a significant increase in the vortioxetine group compared with the vehicle and fluoxetine groups. (C) The number of mitochondria in dendrites was not significantly different in the vortioxetine group compared with the vehicle and fluoxetine groups. (D) The mean volume of mitochondria in CA1 stratum radiatum was not significantly different in the vortioxetine group compared with the vehicle and fluoxetine groups.

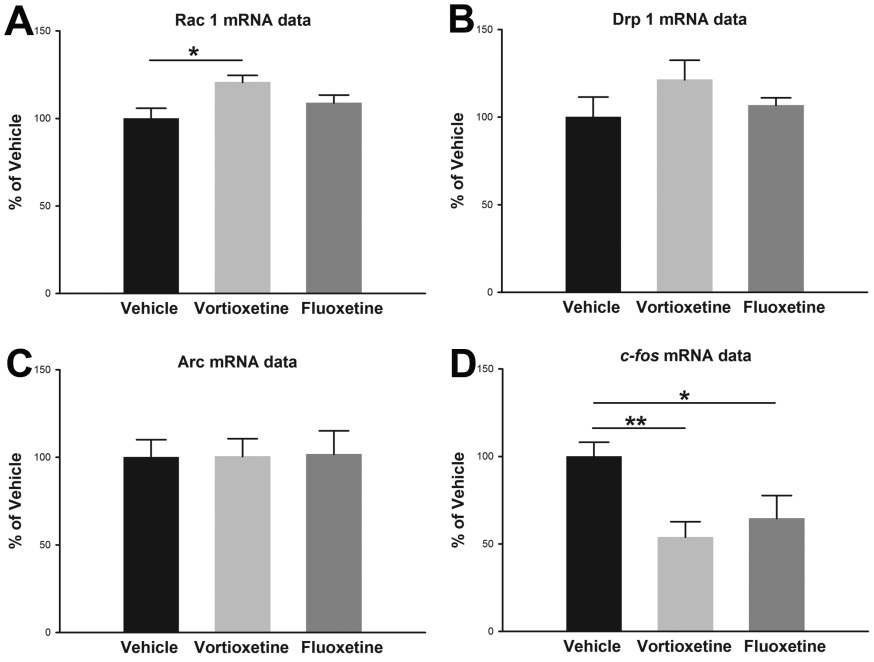

Figure 6. mRNA expression investigated with real-time qPCR after 1-week treatment with fluoxetine and vortioxetine. Plotted data show normalized mean group values ± SEM and are expressed as percent of control rats. Asterisks represent significant differences from control rats (*$P < .05$). n = 8 in each group.

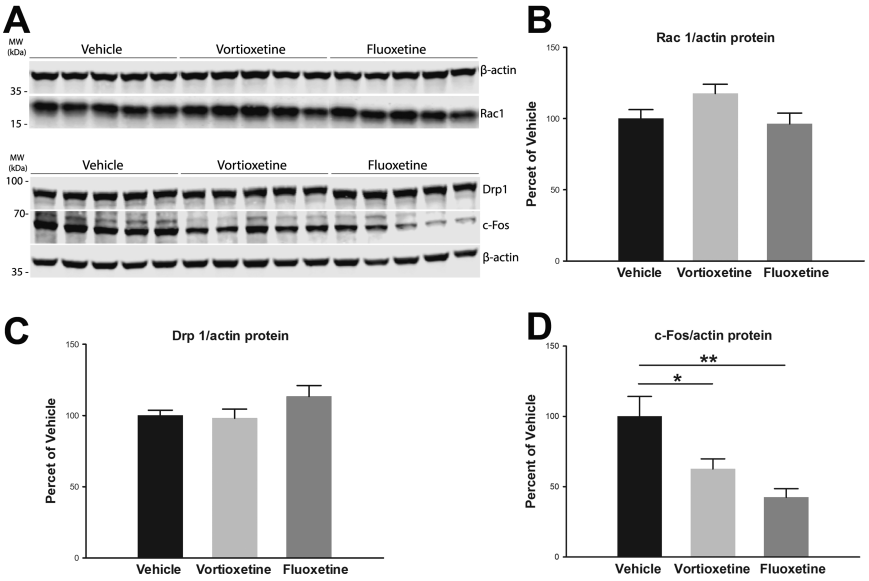

Figure 7. Protein expression levels of Rac1 and Drp1 in hippocampal total lysate. (A) Representative immunoblots of Rac1, Drp1, and c-Fos protein expression in response to vortioxetine and fluoxetine treatment. (B–D) Bar graphs representing the β-actin normalized density of Rac1, Drp1, and c-Fos (n = 8 rats/group). Data are expressed as mean percentage ± SEM of control mean values (*P < .05, **P < .01, 1-way ANOVA followed by Dunnett's test for multiple comparisons).

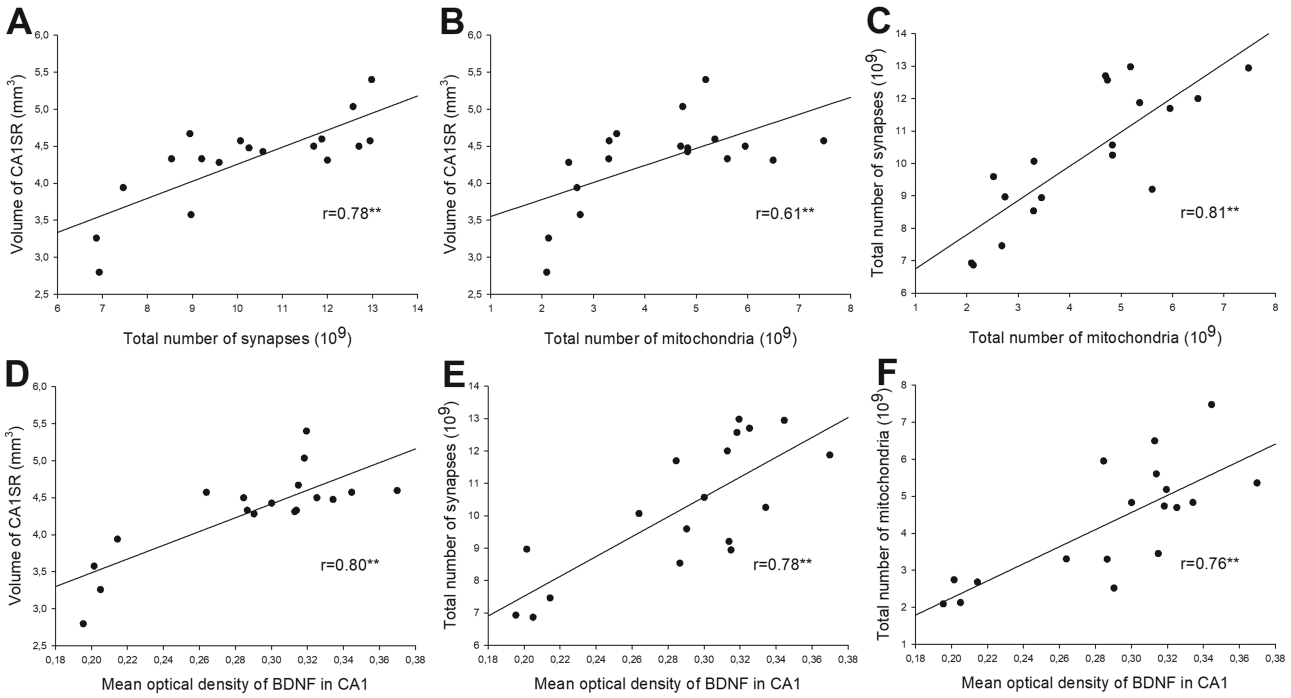

Figure 8. The correlations between BDNF, synaptic plasticity, and mitochondria plasticity of hippocampus (***P < .001). The volume of hippocampal CA1-SR correlated positively with synapse number (A) and mitochondrial number (B). The levels of BDNF expression correlated positively with the volume of hippocampal CA1-SR (D), synapse number (E), and mitochondrial number (F). Furthermore, there was a strong significant positive correlation between the total mitochondria number density and total number of synapses (C).

d treatment. The gene expression level of Rac1 was significantly increased and Drp1 showed a tendency towards an increase in the vortioxetine treatment group. Moreover, there was a tendency towards increase of protein expression levels of Rac1 after vortioxetine treatment by immunoblotting. However, both gene and protein expression levels of c-Fos were significantly decreased. Furthermore, there was a significant positive correlation between BDNF level and mitochondria/synapse number. Based on our previous observation that vortioxetine increases spine number and dendritic branching in the hippocampus CA1 faster than the SSRI fluoxetine, the present study supports the hypothesis that the new spines induced by vortioxetine can rapidly form functional synapses by mitochondrial support, accompanied by increased BDNF-signaling.

Table 1. Summary of the Overall Measurement Results of Ultrastructure

	Vehicle	Vortioxetine	Fluoxetine	Veh vs Vor	Veh vs Flu
				P	*P*
Total volume (hippocampus)	34.870 (6.907)	42.373 (4.162)	35.553 (6.301)	<.05	.86
V(CA1)	3.961 (0.748)	4.736 (0.403)	4.233 (0.393)	<.05	.44
Total N(syn/CA1) x10 (9)	8.684 (1.490)	12.4511 (0.472)	9.498 (1.488)	<.001	.36
N(np-syn) x10 (9)	6.296 (1.135)	8.9710 (1.055)	6.978 (0.907)	<.01	.28
N(p-syn) x10 (9)	1.982 (0.361)	3.027 (0.779)	2.242 (0.907)	<.05	.45
N(sh-syn) x10 (9)	0.406 (0.109)	0.513 (0.1511)	0.277 (0.153)	.11	.12
Total N(mit/CA1) x10 (9)	3.438 (1.483)	5.657 (1.105)	3.802 (1.307)	<.05	.66
N(a-mit)x10 (9)	2.366 (0.957)	3.895 (0.656)	2.752 (1.052)	<.01	.52
N(d-mit)x10 (9)	1.065 (0.521)	1.745 (0.556)	1.048 (0.349)	.05	.95
VN(mit/CA1) μm^3	0.080(0.018)	0.062(0.015)	0.069(0.013)	.11	.29
Total V(mit/CA1) mm^3	0.257(0.071)	0.255(0.012)	0.252(0.043)	<.05	.880

Abbreviations: N(a-mit), number of mitochondria in axons; N(d-mit), number of mitochondria in dendrites; N(mit/CA1), number of mitochondria in CA1; N(np-syn), number of nonperforated synapses; N(p-syn), the number of perforated synapses; N(sh-syn), the number of shaft synapses; N(syn/CA1), total number of synapses in CA1; V(CA1), volume of CA1 stratum radiatum; V(mit/CA1), total volume of mitochondria in CA1; V_N(mit/CA1), mean volume of mitochondria.

Effect of Vortioxetine on Hippocampal Synaptic Plasticity and Synapse-Related Gene Expression

Several lines of evidence suggest that, in addition to neurogenesis, more rapid synaptic plasticity may play an important role in the neurobiology of depression and effects of antidepressant therapy (Popoli et al., 2002; Duman, 2004). The current results showed that the number of synapses (including both nonperforated and perforated synapses) significantly increased in the vortioxetine group compared with the vehicle group. However, there were no changes in the fluoxetine group compared with the vehicle group at this time point. Previously, we have reported that 1-week vortioxetine treatment induced changes in spine number and density and also dendritic morphology, whereas an equivalent dose of fluoxetine had no effects (Chen et al., 2016). Our recent findings implied that induction of synapses was associated with the creation of new spines at adjacent sites in the dendrite. Therefore, the increased number of synapses is correlated with changes of spine number and dendritic morphology. Previous experiments indicated that vortioxetine enhanced LTP in the CA1 subregion of the hippocampus (Dale et al., 2014).

Furthermore, these morphological changes were associated with the improvement of depression-like behavior in the forced swim test (FST) according to our previous behavioral results. Li et al. (Li et al., 2013) used a progesterone withdrawal model in female Long-Evans rats to investigate the effects of several classes of antidepressants (including vortioxetine and fluoxetine) in the FST as a measure of antidepressant activity. Acute (3 injections over 2 days) treatment results showed that vortioxetine significantly reduced immobility in the FST, whereas fluoxetine was ineffective. Therefore, our findings support that synaptic plasticity may play an important role in the effects of antidepressant therapy.

Evidence suggests that Rac1, a well-known Rho GTPase, contributes to the regulation of dendritic spine formation, excitatory synapses, and synaptic function (Penzes et al., 2003; Calabrese et al., 2006; Oh et al., 2010). The longer dendritic spines in hippocampal CA1 pyramidal neurons of Srgap 3-/- mice were found through increasing Rac1 activity by negatively regulating Srgap3 (Waltereit et al., 2012). The definitive evidence showed compelling links between Rho GTPases signaling and cognitive function (De et al., 2014). Zamboni et al. (Zamboni et al., 2016) have also documented a role for Rac-regulators in hippocampal neurogenesis and synaptogenesis and shown that dysregulation leads to cognitive impairment. Thus, Rho GTPases and their downstream effectors may represent important therapeutic targets for disorders associated with cognitive dysfunction. Interestingly, the role of Rac1 in modulation of synapses is not limited to hippocampus and reported in other brain regions including nucleus accumbens (Golden et al., 2013). A recent study indicated the impact of vortioxetine on synaptic integration in prefrontal-subcortical circuits by showing diminished mPFC-msNAc afferent drive (Chakroborty et al., 2017).

Emerging findings have suggested that BDNF plays a critical role as a regulator of neuronal development and function, through Rac1-mediated remodeling of the actin cytoskeleton (Zhou et al., 2007) and the defect in BDNF-induced spine morphogenesis is a result of impaired activation of Rac1 (Lai et al., 2012). Consistent with these findings, our results indicate that the morphological changes of synapses to some extent may rely on Rac1-dependent signaling cascade accompanied by BDNF elevation.

The IEGs, such as *c-fos*, has been widely used as a molecular marker tightly associated with synaptic plasticity (Minatohara et al., 2015). The transcription factor IEGs *c-fos* is considered as a good candidate for the initial steps of learning inducing long-term synaptic plasticity (Abraham et al., 1991). This indicates that the threshold of synaptic activation inducing the expression of transcription factor genes in particular brain regions can be closely linked to synaptic plasticity. In the present study, *c-fos* was downregulated in response to vortioxetine treatment. Consistent with these results, 4 weeks chronic vortioxetine can promote a decrease in *c-fos* expression in the hippocampus (Waller et al., 2016). Although several lines of evidence reveal that vortioxetine can promote expression of various genes that play a role in synaptic plasticity (Li et al., 2015; du Jardin et al., 2016; Waller et al., 2017), these studies measured mRNA expression and were not focused on a particular layer of hippocampus, as well as by species differences in the response to vortioxetine.

Effect of Vortioxetine on Hippocampal Mitochondrial Plasticity and Mitochondria-Related Gene Expression

Synaptic transmission requires mitochondrial ATP generation for neurotransmitter exocytosis, vesicle recruitment, activation

of ion conductance, signaling at metabotropic receptors, potentiation of neurotransmitter release, and synaptic plasticity (Li et al., 2010; Jiao and Li, 2011). Mitochondrial dynamics, a corporate term for the processes of mitochondrial fission, fusion, and transport, controls mitochondrial function and localization within the cell (Detmer and Chan, 2007). Mitochondria constantly move along axons and dendrites, dividing and fusing in response to synaptic changes (Mattson et al., 2008; Palmer et al., 2011), and help to regulate synaptic activity and consequently learning and memory (Li et al., 2010; Jiao and Li, 2011). Mitochondria, therefore, not only provide dynamic energy support for normal synaptic functioning but also directly modulate synaptic structural and functional plasticity (Cheng et al., 2010). Our results suggest that the increased mitochondrial number provided ATP to support features of synaptogenesis. Therefore, mitochondrial biogenesis may play an important physiological role in synaptic plasticity in the hippocampus.

Mitochondria are dynamically transported in and out of axons and dendrites to maintain neuronal and synaptic function. It is shown that the movement of mitochondria in axons and dendrites are different due to the movement of mitochondria in axons with a consistently rapid velocity than are those in dendrites (Ligon and Steward, 2000). Therefore, the difference in motility and metabolic properties of mitochondria in axons and dendrites reflects alterations in energy metabolism during synaptic plasticity. Since most metabolic activity takes place in axon terminals (Zinsmaier et al., 2009), an increased number of mitochondria in axon terminals after vortioxetine treatment in our study implies that the increased metabolism may support high synaptic activity by the generation of action potentials and trafficking of synaptic vesicles (neurotransmitter exocytosis and vesicle recruitment).

Regulation of mitochondrial dynamics is partly accomplished through posttranslational modification of mitochondrial fission and fusion enzymes, in turn influencing mitochondrial bioenergetics and transport (Cheng et al., 2010). The importance of posttranslational regulation is highlighted in numerous neurodegenerative disorders associated with posttranslational modification of the mitochondrial fission enzyme Drp1 (Li et al., 2004). One study showed that mitochondrial abnormality including morphological impairment is due to the imbalance between mitochondrial fusion and fission via a glycogen synthase kinase 3β (GSK3β)/dynamin-related protein-1 (Drp1)-dependent mechanism (Huang et al., 2015).

Furthermore, increasing mitochondrial fragmentation by overexpression of Drp1 enhances synapse formation, whereas dominant-negative inhibition of Drp1 has the opposite effect in cultured hippocampal neurons, indicating a prominent role for mitochondrial dynamics in synaptogenesis (Dickey and Strack, 2011). Our finding showing a tendency towards increased levels of Drp1 gene is consistent with their findings. But, there was no significant change of protein levels of Drp1. However, it was not certain whether a vortioxetine-induced increase in Drp1 gene expression was associated with a similar enhancement on protein level of Drp1 and the functional activity of the protein. Moreover, correlation analysis in large-scale data sets reported approximately 50% correspondence between messenger RNA and protein levels (Tian et al., 2004). Thus, the gene expression of Drp1 in the present study may possibly offer a mechanistic explanation for increased mitochondria number induced by vortioxetine. Furthermore, a link between Drp1 and mitochondria plasticity may indicate that there is an increase of mitochondrial fission after vortioxetine treatment.

Interestingly, several studies have demonstrated that fluoxetine induces mitochondria triggering apoptosis and/or interferes with mitochondrial function by modulating the activity of respiratory chain components and enzymes of the Krebs cycle. Furthermore, fluoxetine alters mitochondria-related redox aspects in different experimental models (de Oliveira, 2016). However, there was no significant effect of fluoxetine on hippocampal mitochondrial plasticity and mitochondria-related genes expression in this study. This discrepancy may be explained by the fact that the dosage and time of fluoxetine administration in the present study was different compared with the previous reports (Adzic et al., 2013).

5-HT Receptor Activities of Vortioxetine

Recent studies demonstrated that vortioxetine prevented the 5-HT-induced increase in inhibitory post-synaptic potentials recorded from CA1 pyramidal cells, most likely by 5-HT_3 receptor antagonism (Dale et al., 2014). Furthermore, 5-HT_3 receptor antagonists exhibited memory-enhancing properties in a number of preclinical cognition models (Arnsten et al., 1997; Pitsikas and Borsini, 1996). A selective 5-HT_{1A}R agonist (flesinoxan) and a selective 5-HT_3 receptor antagonist (ondansetron) reversed memory impairments in 5-HT depleted rats (Jensen et al., 2014). Thus, accumulating evidence suggests that both 5-HT_{1A} and 5-HT_3 receptors play an important role in the effect of vortioxetine on cognitive function.

A selective 5-HT_3 receptor antagonist, Tropisetron, protected PC12 cells against high glucose-induced apoptosis and oxidative stress by preventing mitochondrial pathways (Aminzadeh, 2017). Oxidative stress results from an imbalance between the production of ROS and antioxidant capacity (Uttara et al., 2009). ROS could increase the gating potential of mitochondrial pores and contribute to cytochrome c release (Sharifi et al., 2007). The 5-HT_{1A} receptor agonist promoted axonal transport of mitochondria in hippocampus neurons by activating the Akt- GSK3β pathway (Chen et al., 2007). GSK3β is a common therapeutic target of many antidepressant drugs (Jope and Roh, 2006). Thus, it is suggested that aberrant 5-HT-induced mitochondrial movement may be linked to depression, and effects of 5-HT on mitochondria functionality may be mediated by both 5-HT_{1A} and 5-HT_3 receptors. Furthermore, we suggest that vortioxetine's 5-HT_{1A} receptor agonism and 5-HT_3 receptor antagonism may contribute to cognitive function through mitochondrial biogenesis based on our present findings.

The Relationship between BDNF, Synaptic Plasticity, and Mitochondria Plasticity of Hippocampus in Depression

Emerging findings suggest roles for mitochondria as mediators of at least some of the effects of glutamate and BDNF on synaptic plasticity (Shuttleworth et al., 2003; Lu et al., 2009). Several neurotrophic factors including BDNF have been shown to promote neuronal differentiation, survival, and modifying synaptic plasticity (Duman and Monteggia, 2006; Kermani and Hempstead, 2007). BDNF promotes synaptic transmission and plasticity, in part by increasing mitochondrial energy production (Markham et al., 2014). Consequences of abnormalities in the BDNF and glucocorticoid receptor signaling are impairment of mitochondrial respiration efficiency and synaptic plasticity (Jeanneteau and Arango-Lievano, 2016). A study of BNDF-induced mitochondrial motility arrest and presynaptic docking suggests that mitochondrial transport and distribution play

an essential role in BDNF-mediated synaptic transmission (Su et al., 2014). The neuroprotective effect of BDNF shares molecular signaling pathways (MEK-Bcl-2 pathway) with mitochondrial respiratory coupling (Markham et al., 2012).

More importantly, the ability of mitochondria in regulation of Ca^{2+} clearance in connection with BDNF signaling pathways is a key point of modulating the synaptic plasticity, especially synaptogenesis (Markham et al., 2014). Consistent with these findings, our results also indicated that BDNF has a significant positive correlation with synapse and mitochondrial number.

The mitochondria are essential components in synaptic transmission, since they are a major source of energy required for maintenance and restoration of ion gradients (Todorova and Blokland, 2017). High levels of monocarboxylate (Gerhart et al., 1998) and glucose (Gerhart et al., 1991) transporters have been observed in CA1, suggesting elevated metabolic and synaptic activity. Several studies suggest that physical proximity between mitochondria and synapses is regulated by neuronal activity (Courchet et al., 2013; Sheng, 2014). Our results showed that increased total synapse numbers are strongly positively correlated with total mitochondria number. The mitochondrial changes may be crucially linked to changed energy metabolism and, therefore, may have consequences for cell plasticity, resilience, and survival in patients with MDD. Antidepressants might ultimately enhance energy metabolism and reduce the damage of oxidative stress. However, because our experimental model is in vivo, it is difficult to show directly the role of mitochondria in synaptic plasticity. Further in vitro studies would be necessary to elucidate how mitochondria modulate synaptic plasticity, e.g., changes of dendritic mitochondria content or mitochondrial activity.

In conclusion, our study suggests that mitochondria play a critical role in synaptic plasticity accompanied by increasing BDNF levels. In particular, the coincidence of rapid changes in the BDNF levels and synaptic/mitochondria plasticity of hippocampus following vortioxetine compared with fluoxetine may be ascribed to vortioxetine's modulation of one or more serotonin receptors. A newly published patent (US 9820984 B1) documents that a treatment regimen of a single i.v. dose of vortioxetine followed by oral vortioxetine achieves a faster onset of therapeutic action in MDD patients (Sanchez et al., 2017). Further studies are necessary to clarify how BDNF levels trigger changes in mitochondria and synapses. These findings might provide insights in to how to target specific 5-HT receptors to induce mitochondrial biogenesis and may provide new avenues for development of novel therapeutics targeting the biogenesis response.

Supplementary Material

Supplementary data are available at *International Journal of Neuropsychopharmacology* online.

Acknowledgments

Herdis Krunderup and Lone Lysgaard are gratefully acknowledged for their skillful EM technical assistance.

Statement of Interest

Dr. Chen reports having received salary support from H. LundbeckA/S. Dr. Ardalan reported having salary support from Lundbeck Foundation. Connie Sanchez was full-time employee at H. Lundbeck A/S when the study was conducted. Dr. Nyengaard reports having received research funding from Sino-Danish Center and the Villum Foundation via Centre for Stochastic Geometry and Advanced Bioimaging. Dr. Wegener reported having received lecture/consultancy fees from H. Lundbeck A/S, Servier SA, Astra Zeneca AB, Eli Lilly A/S, Sun Pharma Pty Ltd, Pfizer Inc, Shire A/S, HB Pharma A/S, Arla Foods A.m.b.A., Alkermes Inc, and Mundipharma International Ltd., and research funding from the Danish Medical Research Council, Aarhus University Research Foundation (AU-IDEAS initiative (eMOOD)), the Novo Nordisk Foundation, the Lundbeck Foundation, and EU Horizon 2020 (ExEDE). Drs Ardalan, Danladi, Elfving and Müller reported no biomedical financial interests or potential conflicts of interest.

References

Abraham WC, Dragunow M, Tate WP (1991) The role of immediate early genes in the stabilization of long-term potentiation. Mol Neurobiol 5:297–314.

Adzic M, Lukic I, Mitic M, Djordjevic J, Elaković I, Djordjevic A, Krstic-Demonacos M, Matić G, Radojcic M (2013) Brain region- and sex-specific modulation of mitochondrial glucocorticoid receptor phosphorylation in fluoxetine treated stressed rats: effects on energy metabolism. Psychoneuroendocrinology 38:2914–2924.

Alcocer-Gómez E, de Miguel M, Casas-Barquero N, Núñez-Vasco J, Sánchez-Alcazar JA, Fernández-Rodríguez A, Cordero MD (2014) NLRP3 inflammasome is activated in mononuclear blood cells from patients with major depressive disorder. Brain Behav Immun 36:111–117.

Aminzadeh A (2017) Protective effect of tropisetron on high glucose induced apoptosis and oxidative stress in PC12 cells: roles of JNK, P38 mapks, and mitochondria pathway. Metab Brain Dis 32:819–826.

Andersen CL, Jensen JL, Ørntoft TF (2004) Normalization of real-time quantitative reverse transcription-PCR data: a model-based variance estimation approach to identify genes suited for normalization, applied to bladder and colon cancer data sets. Cancer Res 64:5245–5250.

Anderson G (2018) Linking the biological underpinnings of depression: role of mitochondria interactions with melatonin, inflammation, sirtuins, tryptophan catabolites, DNA repair and oxidative and nitrosative stress, with consequences for classification and cognition. Prog Neuropsychopharmacol Biol Psychiatry 80:255–266.

Arnsten AF, Lin CH, Van Dyck CH, Stanhope KJ (1997) The effects of 5-HT3 receptor antagonists on cognitive performance in aged monkeys. Neurobiol Aging 18:21–28.

Bonefeld BE, Elfving B, Wegener G (2008) Reference genes for normalization: a study of rat brain tissue. Synapse 62:302–309.

Calabrese B, Wilson MS, Halpain S (2006) Development and regulation of dendritic spine synapses. Physiology (Bethesda) 21:38–47.

Chakroborty S, Geisbush TR, Dale E, Pehrson AL, Sánchez C, West AR (2017) Impact of vortioxetine on synaptic integration in prefrontal-subcortical circuits: comparisons with escitalopram. Front Pharmacol 8:764.

Chang DT, Honick AS, Reynolds IJ (2006) Mitochondrial trafficking to synapses in cultured primary cortical neurons. J Neurosci 26:7035–7045.

Chen F, Madsen TM, Wegener G, Nyengaard JR (2010) Imipramine treatment increases the number of hippocampal synapses and neurons in a genetic animal model of depression. Hippocampus 20:1376–1384.

Chen F, Wegener G, Madsen TM, Nyengaard JR (2013) Mitochondrial plasticity of the hippocampus in a genetic rat

model of depression after antidepressant treatment. Synapse 67:127–134.
Chen F, du Jardin KG, Waller JA, Sanchez C, Nyengaard JR, Wegener G (2016) Vortioxetine promotes early changes in dendritic morphology compared with fluoxetine in rat hippocampus. Eur Neuropsychopharmacol 26:234–245.
Chen S, Owens GC, Crossin KL, Edelman DB (2007) Serotonin stimulates mitochondrial transport in hippocampal neurons. Mol Cell Neurosci 36:472–483.
Cheng A, Hou Y, Mattson MP (2010) Mitochondria and neuroplasticity. ASN Neuro 2:e00045.
Courchet J, Lewis TL Jr, Lee S, Courchet V, Liou DY, Aizawa S, Polleux F (2013) Terminal axon branching is regulated by the LKB1-NUAK1 kinase pathway via presynaptic mitochondrial capture. Cell 153:1510–1525.
Czarny P, Wigner P, Galecki P, Sliwinski T (2018) The interplay between inflammation, oxidative stress, DNA damage, DNA repair and mitochondrial dysfunction in depression. Prog Neuropsychopharmacol Biol Psychiatry 80:309–321.
Dale E, Zhang H, Leiser SC, Xiao Y, Lu D, Yang CR, Plath N, Sanchez C (2014) Vortioxetine disinhibits pyramidal cell function and enhances synaptic plasticity in the rat hippocampus. J Psychopharmacol 28:891–902.
De Filippis B, Romano E, Laviola G (2014) Aberrant rho gtpases signaling and cognitive dysfunction: in vivo evidence for a compelling molecular relationship. Neurosci Biobehav Rev 46:285–301.
de Oliveira MR (2016) Fluoxetine and the mitochondria: a review of the toxicological aspects. Toxicol Lett 258:185–191.
Detmer SA, Chan DC (2007) Functions and dysfunctions of mitochondrial dynamics. Nat Rev Mol Cell Biol 8:870–879.
Dickey AS, Strack S (2011) PKA/AKAP1 and PP2A/bβ2 regulate neuronal morphogenesis via drp1 phosphorylation and mitochondrial bioenergetics. J Neurosci 31:15716–15726.
du Jardin KG, Müller HK, Sanchez C, Wegener G, Elfving B (2016) A single dose of vortioxetine, but not ketamine or fluoxetine, increases plasticity-related gene expression in the rat frontal cortex. Eur J Pharmacol 786:29–35.
Duman RS (2004) Neural plasticity: consequences of stress and actions of antidepressant treatment. Dialogues Clin Neurosci 6:157–169.
Duman RS, Monteggia LM (2006) A neurotrophic model for stress-related mood disorders. Biol Psychiatry 59:1116–1127.
Elfving B, Bonefeld BE, Rosenberg R, Wegener G (2008) Differential expression of synaptic vesicle proteins after repeated electroconvulsive seizures in rat frontal cortex and hippocampus. Synapse 62:662–670.
Elfving B, Plougmann PH, Wegener G (2010) Differential brain, but not serum VEGF levels in a genetic rat model of depression. Neurosci Lett 474:13–16.
Frampton JE (2016) Vortioxetine: a review in cognitive dysfunction in depression. Drugs 76:1675–1682.
Geinisman Y, Berry RW, Disterhoft JF, Power JM, Van der Zee EA (2001) Associative learning elicits the formation of multiple-synapse boutons. J Neurosci 21:5568–5573.
Gerhart DZ, Djuricic B, Drewes LR (1991) Quantitative immunocytochemistry (image analysis) of glucose transporters in the normal and postischemic rodent hippocampus. J Cereb Blood Flow Metab 11:440–448.
Gerhart DZ, Enerson BE, Zhdankina OY, Leino RL, Drewes LR (1998) Expression of the monocarboxylate transporter MCT2 by rat brain glia. Glia 22:272–281.
Golden SA, Christoffel DJ, Heshmati M, Hodes GE, Magida J, Davis K, Cahill ME, Dias C, Ribeiro E, Ables JL, Kennedy PJ, Robison AJ, Gonzalez-Maeso J, Neve RL, Turecki G, Ghose S, Tamminga CA, Russo SJ (2013) Epigenetic regulation of RAC1 induces synaptic remodeling in stress disorders and depression. Nat Med 19:337–344.
Huang S, Wang Y, Gan X, Fang D, Zhong C, Wu L, Hu G, Sosunov AA, McKhann GM, Yu H, Yan SS (2015) Drp1-mediated mitochondrial abnormalities link to synaptic injury in diabetes model. Diabetes 64:1728–1742.
Jeanneteau F, Arango-Lievano M (2016) Linking mitochondria to synapses: new insights for stress-related neuropsychiatric disorders. Neural Plast 2016:3985063.
Jensen JB, du Jardin KG, Song D, Budac D, Smagin G, Sanchez C, Pehrson AL (2014) Vortioxetine, but not escitalopram or duloxetine, reverses memory impairment induced by central 5-HT depletion in rats: evidence for direct 5-HT receptor modulation. Eur Neuropsychopharmacol 24:148–159.
Jiao S, Li Z (2011) Nonapoptotic function of BAD and BAX in long-term depression of synaptic transmission. Neuron 70:758–772.
Jope RS, Roh MS (2006) Glycogen synthase kinase-3 (GSK3) in psychiatric diseases and therapeutic interventions. Curr Drug Targets 7:1421–1434.
Kermani P, Hempstead B (2007) Brain-derived neurotrophic factor: a newly described mediator of angiogenesis. Trends Cardiovasc Med 17:140–143.
Klinedinst NJ, Regenold WT (2015) A mitochondrial bioenergetic basis of depression. J Bioenerg Biomembr 47:155–171.
Kroustrup JP, Gundersen HJ (2001) Estimating the number of complex particles using the conneulor principle. J Microsc 203:314–320.
Lai KO, Wong AS, Cheung MC, Xu P, Liang Z, Lok KC, Xie H, Palko ME, Yung WH, Tessarollo L, Cheung ZH, Ip NY (2012) Trkb phosphorylation by cdk5 is required for activity-dependent structural plasticity and spatial memory. Nat Neurosci 15:1506–1515.
Li Y, Raaby KF, Sánchez C, Gulinello M (2013) Serotonergic receptor mechanisms underlying antidepressant-like action in the progesterone withdrawal model of hormonally induced depression in rats. Behav Brain Res 256:520–528.
Li Y, Abdourahman A, Tamm JA, Pehrson AL, Sánchez C, Gulinello M (2015) Reversal of age-associated cognitive deficits is accompanied by increased plasticity-related gene expression after chronic antidepressant administration in middle-aged mice. Pharmacol Biochem Behav 135:70–82.
Li Y, Sanchez C, Gulinello M (2017) Distinct antidepressant-like and cognitive effects of antidepressants with different mechanisms of action in middle-aged female mice. Int J Neuropsychopharmacol 20:510–515.
Li Z, Okamoto K, Hayashi Y, Sheng M (2004) The importance of dendritic mitochondria in the morphogenesis and plasticity of spines and synapses. Cell 119:873–887.
Li Z, Jo J, Jia JM, Lo SC, Whitcomb DJ, Jiao S, Cho K, Sheng M (2010) Caspase-3 activation via mitochondria is required for long-term depression and AMPA receptor internalization. Cell 141:859–871.
Ligon LA, Steward O (2000) Movement of mitochondria in the axons and dendrites of cultured hippocampal neurons. J Comp Neurol 427:340–350.
Lu CW, Lin TY, Chiang HS, Wang SJ (2009) Facilitation of glutamate release from rat cerebral cortex nerve terminal by subanesthetic concentration propofol. Synapse 63:773–781.
Markham A, Cameron I, Bains R, Franklin P, Kiss JP, Schwendimann L, Gressens P, Spedding M (2012) Brain-derived neurotrophic factor-mediated effects on mitochondrial respiratory

coupling and neuroprotection share the same molecular signalling pathways. Eur J Neurosci 35:366–374.
Markham A, Bains R, Franklin P, Spedding M (2014) Changes in mitochondrial function are pivotal in neurodegenerative and psychiatric disorders: how important is BDNF? Br J Pharmacol 171:2206–2229.
Mattson MP, Gleichmann M, Cheng A (2008) Mitochondria in neuroplasticity and neurological disorders. Neuron 60:748–766.
Minatohara K, Akiyoshi M, Okuno H (2015) Role of immediate-early genes in synaptic plasticity and neuronal ensembles underlying the memory trace. Front Mol Neurosci 8:78.
Oh D, et al. (2010) Regulation of synaptic rac1 activity, long-term potentiation maintenance, and learning and memory by BCR and ABR rac gtpase-activating proteins. J Neurosci 30:14134–14144.
Palmer CS, Osellame LD, Stojanovski D, Ryan MT (2011) The regulation of mitochondrial morphology: intricate mechanisms and dynamic machinery. Cell Signal 23:1534–1545.
Pan Z, Grovu RC, Cha DS, Carmona NE, Subramaniapillai M, Shekotikhina M, Rong C, Lee Y, McIntyre RS (2017) Pharmacological treatment of cognitive symptoms in major depressive disorder. CNS Neurol Disord Drug Targets 16:891–899.
Pehrson AL, Hillhouse TM, Haddjeri N, Rovera R, Porter JH, Mørk A, Smagin G, Song D, Budac D, Cajina M, Sanchez C (2016) Task- and treatment length-dependent effects of vortioxetine on scopolamine-induced cognitive dysfunction and hippocampal extracellular acetylcholine in rats. J Pharmacol Exp Ther 358:472–482.
Penzes P, Beeser A, Chernoff J, Schiller MR, Eipper BA, Mains RE, Huganir RL (2003) Rapid induction of dendritic spine morphogenesis by trans-synaptic ephrinb-ephb receptor activation of the rho-GEF kalirin. Neuron 37:263–274.
Pitsikas N, Borsini F (1996) Itasetron (DAU 6215) prevents age-related memory deficits in the rat in a multiple choice avoidance task. Eur J Pharmacol 311:115–119.
Popoli M, Gennarelli M, Racagni G (2002) Modulation of synaptic plasticity by stress and antidepressants. Bipolar Disord 4:166–182.
Sanchez C, Asin KE, Artigas F (2015) Vortioxetine, a novel antidepressant with multimodal activity: review of preclinical and clinical data. Pharmacol Ther 145:43–57.
Sanchez C, Søby KK, Bang-Andersen B (2017) Dosing regimens for fast onset of antidepressant effect. *United States Patent* US 9820984 B1 Nov. 21, 2017.
Sharifi K, Mostaghni K, Maleki M, Badiei K (2007) Ischaemia/reperfusion injury in experimentally induced abomasal volvulus in sheep. Vet Res Commun 31:575–590.
Sheng ZH (2014) Mitochondrial trafficking and anchoring in neurons: new insight and implications. J Cell Biol 204:1087–1098.
Shuttleworth CW, Brennan AM, Connor JA (2003) NAD(P)H fluorescence imaging of postsynaptic neuronal activation in murine hippocampal slices. J Neurosci 23:3196–3208.
Silva Pereira V, Elfving B, Joca SRL, Wegener G (2017) Ketamine and aminoguanidine differentially affect Bdnf and Mtor gene expression in the prefrontal cortex of adult male rats. Eur J Pharmacol 815:304–311.
Small JV (1968) Measurement of section thickness. [Fourth European Conference on Electron Microscopy]:609–610.
Smith J, Browning M, Conen S, Smallman R, Buchbjerg J, Larsen KG, Olsen CK, Christensen SR, Dawson GR, Deakin JF, Hawkins P, Morris R, Goodwin G, Harmer CJ (2017) Vortioxetine reduces BOLD signal during performance of the N-back working memory task: a randomised neuroimaging trial in remitted depressed patients and healthy controls. Mol Psychiatry.
Su B, Ji YS, Sun XL, Liu XH, Chen ZY (2014) Brain-derived neurotrophic factor (BDNF)-induced mitochondrial motility arrest and presynaptic docking contribute to BDNF-enhanced synaptic transmission. J Biol Chem 289:1213–1226.
Tian Q, Stepaniants SB, Mao M, Weng L, Feetham MC, Doyle MJ, Yi EC, Dai H, Thorsson V, Eng J, Goodlett D, Berger JP, Gunter B, Linseley PS, Stoughton RB, Aebersold R, Collins SJ, Hanlon WA, Hood LE (2004) Integrated genomic and proteomic analyses of gene expression in mammalian cells. Mol Cell Proteomics 3:960–969.
Todorova V, Blokland A (2017) Mitochondria and synaptic plasticity in the mature and aging nervous system. Curr Neuropharmacol 15:166–173.
Uttara B, Singh AV, Zamboni P, Mahajan RT (2009) Oxidative stress and neurodegenerative diseases: a review of upstream and downstream antioxidant therapeutic options. Curr Neuropharmacol 7:65–74.
Vavakova M, Durackova Z, Trebaticka J (2015) Markers of oxidative stress and neuroprogression in depression disorder. Oxid Med Cell Longev 2015:898393.
Waller JA, Chen F, Sánchez C (2016) Vortioxetine promotes maturation of dendritic spines in vitro: a comparative study in hippocampal cultures. Neuropharmacology 103:143–154.
Waller JA, Tamm JA, Abdourahman A, Pehrson AL, Li Y, Cajina M, Sánchez C (2017) Chronic vortioxetine treatment in rodents modulates gene expression of neurodevelopmental and plasticity markers. Eur Neuropsychopharmacol 27:192–203.
Waltereit R, et al (2012) Srgap3$^{-/-}$ mice present a neurodevelopmental disorder with schizophrenia-related intermediate phenotypes. Faseb J 26:4418–4428.
Zamboni V, Armentano M, Sarò G, Ciraolo E, Ghigo A, Germena G, Umbach A, Valnegri P, Passafaro M, Carabelli V, Gavello D, Bianchi V, D'Adamo P, de Curtis I, El-Assawi N, Mauro A, Priano L, Ferri N, Hirsch E, Merlo GR (2016) Disruption of arhgap15 results in hyperactive rac1, affects the architecture and function of hippocampal inhibitory neurons and causes cognitive deficits. Sci Rep 6:34877.
Zhou P, Porcionatto M, Pilapil M, Chen Y, Choi Y, Tolias KF, Bikoff JB, Hong EJ, Greenberg ME, Segal RA (2007) Polarized signaling endosomes coordinate BDNF-induced chemotaxis of cerebellar precursors. Neuron 55:53–68.
Zinsmaier KE, Babic M, Russo GJ (2009) Mitochondrial transport dynamics in axons and dendrites. Results Probl Cell Differ 48:107–139.